

# Effects of Temperature and Strain Rate on the Tensile Behavior of Unfilled and Talc-Filled Polypropylene. Part II: Constitutive Equation

YUANXIN ZHOU and P. K. MALLICK

*Center for Lightweighting Automotive Materials and Processing  
University of Michigan—Dearborn  
Dearborn, Michigan 48128*

Based on the experimental results presented in Part I of this research, a three-parameter nonlinear constitutive model has been proposed to describe the strain rate and temperature dependent tensile behaviors of unfilled and talc-filled polypropylene. One of the parameters is the elastic modulus. The other two parameters in this model are a strain exponent,  $m$ , and a compliance factor,  $\beta$ . Their relationships to strain rate and temperature are obtained from the experimental results. The simulated stress-strain curves from the model are in good agreement with the test data. The analysis of the model shows that the strain exponent  $m$ , which controls the strain softening (or hardening) effect of the material, is not only strain rate independent, but also temperature independent. The compliance parameter,  $\beta$ , which controls the flow stress level of the material, on the other hand, varies with both strain rate as well as temperature. Results also show that the addition of talc filler in polypropylene reduces the strain exponent  $m$ , and increase the compliance parameter,  $\beta$ , which reduces the flow stress level of talc-filled polypropylene to lower than that of unfilled polypropylene.

## 1. INTRODUCTION

Mechanical behavior of semicrystalline thermoplastics and their composites has been the subject of numerous studies over the last few years. The majority of these research efforts have relied on experimental techniques to understand the deformation characteristics of these materials. For example, Hartmann *et al.* (1) reported the tensile yield in polypropylene at different temperatures. Arruda *et al.* (2) examined the deformation characteristics of semicrystalline polypropylene under compressive load at different strain rates.

On the other hand, computer simulations are now used extensively to predict the response of complex structures to mechanical and thermal loads. In order to obtain realistic results from these simulations, constitutive equations are needed that can describe the stress-strain behavior of polymers over a range of strains, strain rates and temperatures. Several recent studies have attempted to formulate an accurate constitutive relationship for semicrystalline polymers. For example, G'Sell and his co-workers (3) have proposed a four-parameter constitutive equation based on tensile test results of round extruded polypropylene specimens. Their constitutive equation utilizes effective stress and effective strain and is applicable to strain

hardening characteristics of the polypropylene investigated. Amoedo *et al.* (4) established a nonlinear viscoplastic model to predict the strain rate and temperature dependent strain hardening behavior of both amorphous and semi-crystalline polymers. Kitagawa *et al.* (5) have used the overstress theory, originally proposed for metals, to simulate the torsional stress-strain characteristics of polypropylene; however, this theory is applicable provided the current strain is not below the maximum previous strain, i.e., for strain-hardening materials. Zhang *et al.* (6) presented two uniaxial constitutive models to characterize the mechanical response of high-density polyethylene. One of them is based on the overstress theory, while the other is a nonlinear viscoelastic model based on a spring in series with six Kelvin spring-dashpot combinations. The parameters in their second models are determined using creep tests.

Experimental results presented in Part I of this research (7) show that both unfilled polypropylene and talc-filled polypropylene are typical strain rate and temperature dependent materials. In the present paper, a three-parameter nonlinear constitutive model will be established to describe the strain rate and temperature dependent tensile behavior of semi-crystalline

polymers. The constitutive model is then applied to unfilled polypropylene and talc-filled polypropylene to predict their tensile stress-strain behavior. It is shown that the proposed model can be used to predict both strain hardening and strain softening characteristics of polymers.

## 2. CONSTITUTIVE EQUATION

Many polymers exhibit nonlinear stress-strain characteristics at stress levels that are lower than the yield strength. The degree of nonlinearity in the stress-strain characteristics depends on both strain rate and temperature. Furthermore, the post-yield behavior may be either strain-hardening, strain-softening or strain-neutral type. On unloading, there is a permanent deformation, which may also be time and temperature dependent. In the proposed constitutive model, the total strain is assumed to be composed of an elastic part and an inelastic part,

$$\varepsilon = \varepsilon_e + \varepsilon_i \quad (1)$$

where,  $\varepsilon_e$  and  $\varepsilon_i$  represent the elastic and inelastic strains, respectively. The elastic strain is assumed to be path-independent and related to the elastic modulus of the material. It is expressed as

$$\varepsilon_e = \frac{\sigma}{E(\dot{\varepsilon}, T)} \quad (2)$$

where,  $E$  is elastic modulus of the material, which is a function of both strain rate and temperature, and  $\sigma$  is the stress. The inelastic strain,  $\varepsilon_i$ , is assumed to be a function of both stress and strain in the following way

$$\varepsilon_i = \beta(\dot{\varepsilon}, T) \sigma \varepsilon^m \quad (3)$$

where  $\beta$  represents a compliance function, which depends on both strain rate and temperature, and  $m$  is a strain exponent. Substituting Eqs 2 and 3 into Eq 1 and rearranging, we obtain

$$\sigma = \frac{E(\dot{\varepsilon}, T)\varepsilon}{1 + E(\dot{\varepsilon}, T)\beta(\dot{\varepsilon}, T)\varepsilon^m} \quad (4)$$

From Eq 4, the slope of the stress-strain diagram at any strain  $\varepsilon$  can be written as

$$\frac{d\sigma}{d\varepsilon} = \frac{E + (1 - m)E^2 \beta \varepsilon^m}{[1 + E\beta \varepsilon^m]^2} \quad (5)$$

At relatively small strains,  $E\beta \varepsilon^m \ll 1$  and, from Eq 4,

$$\frac{d\sigma}{d\varepsilon} \approx E.$$

At relatively large strains,  $E\beta \varepsilon^m \gg 1$  and Eq 4 can be simplified as

$$\frac{d\sigma}{d\varepsilon} = \frac{(1 - m)}{\beta} \varepsilon^{-m} \quad (6)$$

Note that when  $m$  is less than 1, the polymer behaves as a strain-hardening material and when  $m$  is greater

than 1, the polymer behaves as a strain-softening material. When  $m = 1$ , the slope of the stress-strain diagram becomes zero and the polymer is strain neutral, i.e., it is neither strain-hardening, nor strain-softening. Thus, Eq 4 can be used to describe either a strain-hardening, strain-softening or strain-neutral behavior by adjusting the value of the strain exponent  $m$ .

Figure 1 shows schematic stress-strain curves with  $m > 1$ ,  $m < 1$  and  $m = 1$ . It can be observed in this figure that  $m$  not only affects the shape of stress-strain curves, but also the flow stress level. The flow stress level increases with increasing  $m$ . The effect of the compliance factor,  $\beta$ , on stress-strain curves is shown in Fig. 2. The flow stress level decreases with increasing  $\beta$ .

## 3. METHOD OF DETERMINING PARAMETERS IN THE CONSTITUTIVE EQUATION

To determine the material parameters in the constitutive equation, Eq 4 is rewritten as follows

$$\frac{\varepsilon}{\sigma} - \frac{1}{E} = \beta(\dot{\varepsilon}, T)\varepsilon^m \quad (7)$$

which, on taking log on both sides, transforms into

$$\ln\left(\frac{\varepsilon}{\sigma} - \frac{1}{E}\right) = \ln \beta + m \ln \varepsilon \quad (8)$$

Equation 8 represents a linear plot of  $\ln\left[\frac{\varepsilon}{\sigma} - \frac{1}{E}\right]$  vs.  $\ln \varepsilon$ . The slope of this linear plot is  $m$  and the intercept at  $\varepsilon = 1$  is  $\ln \beta$ .

For a strain-softening material, the yield strength,  $\sigma_Y$ , and the corresponding yield strain,  $\varepsilon_Y$ , can be determined from Eq 4.

$$\frac{d\sigma}{d\varepsilon} = 0 \quad \text{when } \varepsilon = \varepsilon_Y \quad (9)$$

i. e.,

$$\varepsilon_Y = \left[ \frac{1}{(m - 1)\beta E} \right]^{1/m} \quad (10)$$

and

$$\sigma_Y = \frac{(m - 1)}{m} E \left[ \frac{1}{(m - 1)\beta E} \right]^{1/m} \quad (11)$$

If we rewrite Eqs 10 and 11, we can obtain the values of  $m$  and  $\ln \beta$  as

$$m = \frac{E\varepsilon_Y}{E\varepsilon_Y - \sigma_Y} \quad (12)$$

$$\beta = \frac{1}{(m - 1)E\varepsilon_Y^m} \quad (13)$$

Thus,  $m$  and  $\beta$  can be calculated from the yield strength,  $\sigma_Y$ , yield strain,  $\varepsilon_Y$ , and elastic modulus,  $E$ , of the material as well.

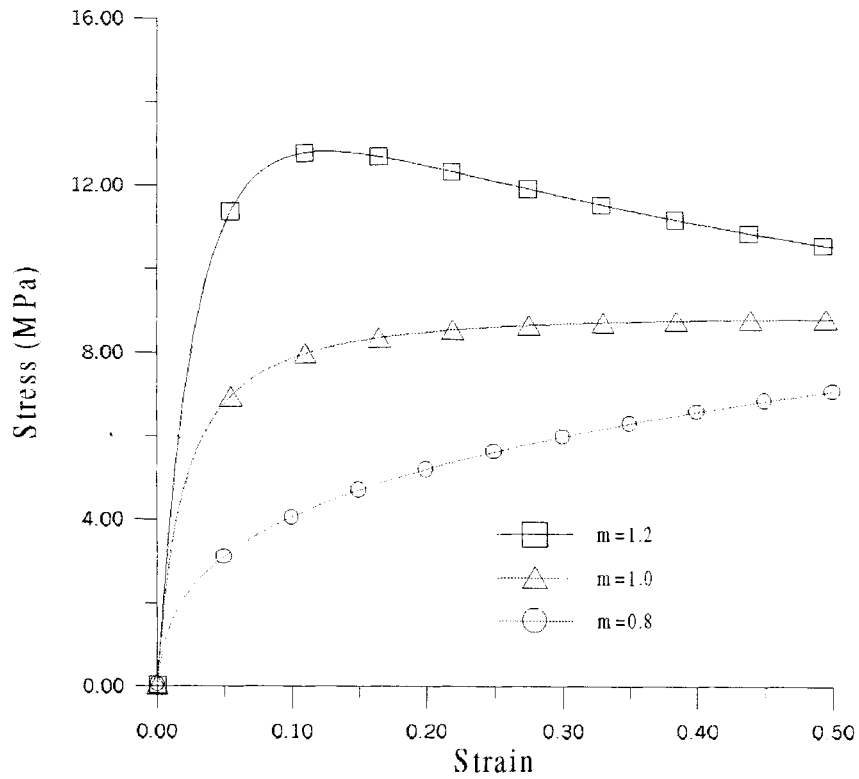


Fig. 1. Schematic representation of the effect of strain exponent,  $m$ , on stress-strain curves.

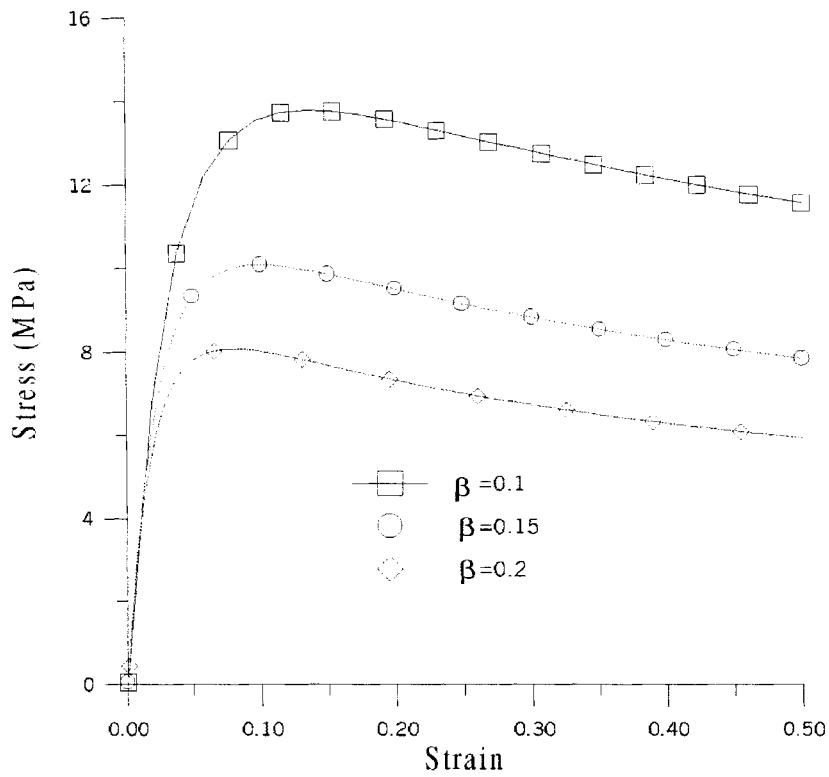


Fig. 2. Schematic representation of the effect of compliance factor,  $\beta$ , on stress-strain curves.

#### 4. TENSILE BEHAVIOR OF POLYPROPYLENE AND 40 W% TALC-FILLED POLYPROPYLENE

In Part I of this research (7), we present the stress-strain diagrams of both polypropylene as well as 40 w% talc-filled polypropylene at four different temperatures, namely 21.5, 50, 75 and 100°C and three different strain rates, namely 0.05, 0.5 and 5 min<sup>-1</sup>. Tensile tests were carried out on specimens machined from 150 mm × 150 mm × 2.5 mm thick injection molded plates parallel to the flow (L) and normal to the flow (W) directions. It was observed that both materials are temperature and strain rate sensitive. Both exhibited non-linearity at stress levels that were lower than the yield strength and decreasing stress level with increasing strain after yielding. The post-yield behavior of these materials can be termed strain-softening. To confirm this behavior, two specimens were first loaded beyond yielding, then unloaded and immediately reloaded until failure occurred. These tests were conducted at 21.5°C and 0.05 min<sup>-1</sup>. The loading-unloading-reloading curves are shown in Fig. 3. In the case of polypropylene, the specimen was unloaded when the strain reached 10%. The unloading took place along a linear path; however, the unloading modulus is 87.5% lower than the initial elastic modulus. The reloading of the polypropylene specimen did not take place along the unloading path and the reloading path was more nonlinear than the initial loading path. The stress-strain diagram of the reloaded specimen did not merge with the initial stress-

strain diagram at the unloading point; however, it did show that the material had strain-softened. Similar strain-softening was also observed for talc-filled polypropylene; however, in this case, the difference between the unloading modulus and the initial modulus is significantly less and the reloading path was very close to the unloading path.

#### 5. ANALYSIS OF THE EXPERIMENTAL RESULTS

Plots of  $\ln\left[\frac{\epsilon}{\sigma} - \frac{1}{E}\right]$  vs.  $\ln\epsilon$  of unfilled polypropylene and 40 w% talc-filled polypropylene in the L directions are shown in Figs. 4 and 5, respectively. As these figures show, these plots are linear at all four temperatures and three strain rates. These linear plots are nearly parallel to each other, which means that each material has the same strain exponent at different test conditions. The compliance factor  $\beta$  and strain exponent  $m$  obtained from these plots and similar plots for the W directions are listed in Tables 1 and 2. These tables also list  $\beta$  and  $m$  calculated from Eqs 12 and 13, respectively. The values of compliance factor  $\beta$  and strain exponent  $m$  derived from the two methods are approximately equal.

From Tables 1 and 2, it can be observed that the strain exponent  $m$  of unfilled polypropylene is greater than that of talc-filled polypropylene, but the compliance factor  $\beta$  of unfilled polypropylene is less than

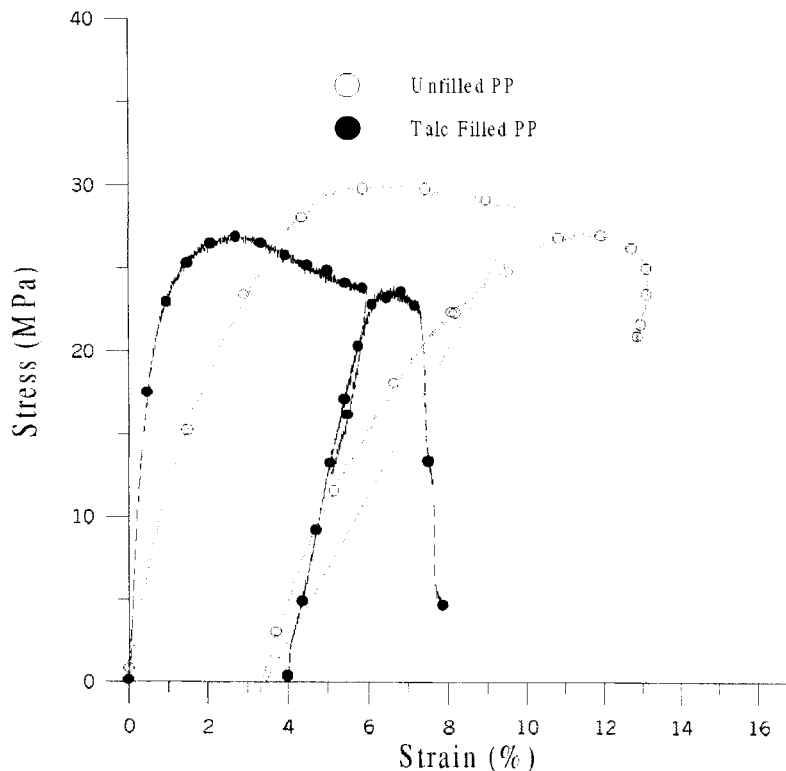


Fig. 3. Loading-unloading-reloading curves of unfilled polypropylene and 40 w% talc-filled polypropylene at 21.5°C and 0.05 min<sup>-1</sup>.

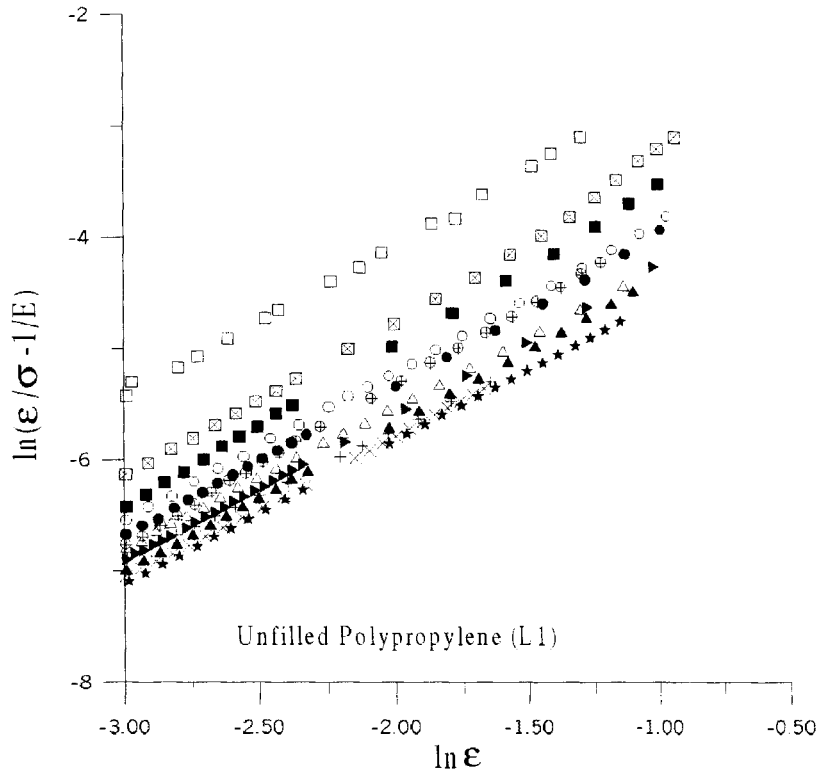


Fig. 4. Plots of  $\ln\left[\frac{\epsilon}{\sigma} - \frac{1}{E}\right]$  vs.  $\ln \epsilon$  for unfilled polypropylene in the flow (L) direction.  $\square$  21.5°C, 0.05 min<sup>-1</sup>;  $\boxtimes$  21.5°C, 0.5 min<sup>-1</sup>;  $\blacksquare$  21.5°C, 5 min<sup>-1</sup>;  $\circ$  50°C, 0.05 min<sup>-1</sup>;  $\bullet$  50°C, 0.5 min<sup>-1</sup>;  $\oplus$  50°C, 5 min<sup>-1</sup>;  $\triangle$  75°C, 0.05 min<sup>-1</sup>;  $\blacktriangleright$  75°C, 0.5 min<sup>-1</sup>;  $\blacktriangle$  75°C, 0.5 min<sup>-1</sup>;  $+$  100°C, 0.05 min<sup>-1</sup>;  $\times$  100°C, 0.5 min<sup>-1</sup>;  $\star$  100°C, 5 min<sup>-1</sup>.

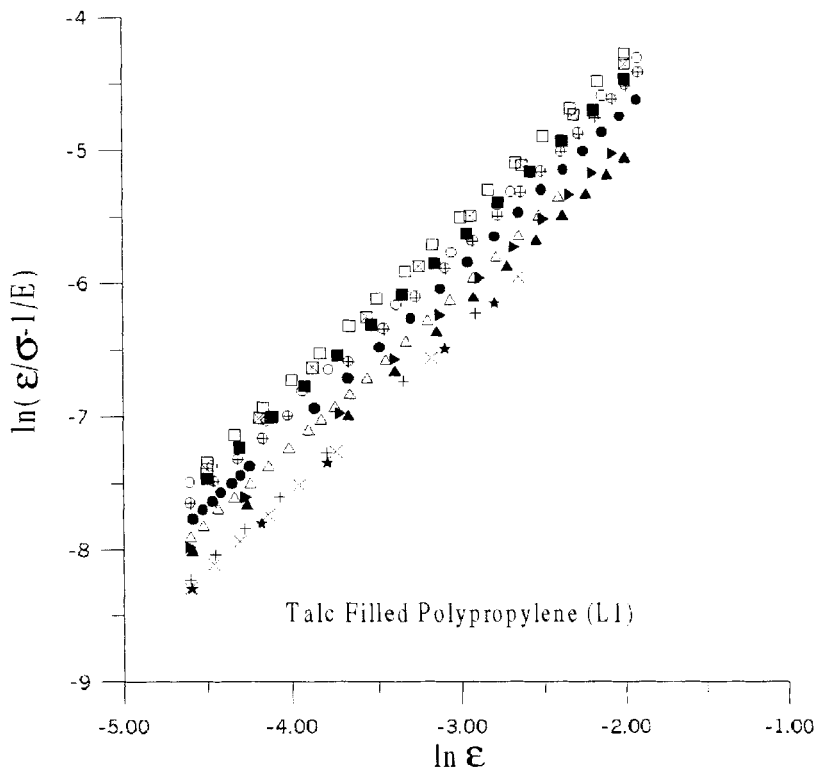


Fig. 5. Plots of  $\ln\left[\frac{\epsilon}{\sigma} - \frac{1}{E}\right]$  vs.  $\ln \epsilon$  for 40 wt% talc-filled polypropylene in the flow (L) direction. The symbols are shown in Fig. 4.

Table 1. Constitutive Parameters of Unfilled Polypropylene.

Strain Rate (min <sup>-1</sup> )	Temp. (°C)	Parallel to the flow direction (L direction)				Normal to the flow direction (W direction)			
		<i>m</i> <sup>a</sup>	$\beta$ <sup>a</sup>	<i>m</i> <sup>b</sup>	$\beta$ <sup>b</sup>	<i>m</i> <sup>a</sup>	$\beta$ <sup>a</sup>	<i>m</i> <sup>b</sup>	$\beta$ <sup>b</sup>
0.05	21.5	1.0016	0.02828	1.2709	0.04072	1.2224	0.06167	1.1996	0.0403
0.5		1.2859	0.03947	1.2804	0.03960	1.2025	0.06559	1.2864	0.0398
5		1.3257	0.04261	1.2726	0.03745	1.3359	0.05752	1.3229	0.0341
0.05	50	1.2719	0.05018	1.3206	0.05652	1.2131	0.07962	1.2091	0.0477
0.5		1.3072	0.05850	1.3203	0.05221	1.2698	0.07663	1.2856	0.0453
5		1.2911	0.04524	1.3281	0.04879	1.2387	0.06822	1.2528	0.0439
0.05	75	1.3238	0.07270	1.3797	0.08286	1.5430	0.1075	1.3901	0.0916
0.5		1.3886	0.07462	1.3591	0.07646	1.5759	0.1092	1.3956	0.0846
5		1.3880	0.07242	1.3517	0.07156	1.3984	0.1009	1.3951	0.0771
0.05	100	1.6568	0.1446	1.4598	0.1491	1.5898	0.1390	1.4212	0.1466
0.5		1.0028	0.6083	1.4110	0.13079	1.5728	0.1076	1.4331	0.1299
5		1.5456	0.1125	1.4417	0.1232	1.4347	0.1071	1.4019	0.1094

<sup>a</sup>Based on Eqs 12 and 13. <sup>b</sup>Based on Eq 8.

that of talc-filled polypropylene, indicating that the talc filler can decrease the flow stress level of polypropylene. The values of  $\beta$  and *m* in the L direction are also different from those in the W direction.

Figures 6–9 show compliance factor  $\beta$  and strain exponent *m* plotted as a function of temperature and strain rate for unfilled polypropylene and 40 w% talc-filled polypropylene in the flow (L) direction. It can be observed from these figures that *m* does not vary much with either temperature or strain rate, and therefore, we consider it to be independent of both strain rate as well as temperature. However, compliance factor  $\beta$  depends on both strain rate as well as temperature. It increases with increasing temperature (Figs. 6 and 7), but decreases with increasing strain rate (Figs. 8 and 9). Similar behavior is also observed normal to flow (W) direction.

The temperature and strain sensitivities of elastic modulus of both polypropylene and 40 w% talc-filled polypropylene are reported in Part I (7). The

expressions of strain exponent *m* and compliance factor  $\beta$  as functions of strain rate and temperature are as follows:

For unfilled polypropylene in the L direction:

$$m = 1.3497$$

$$\beta(1/\text{MPa}) = 0.04523 \left[ 1 - 0.002781 \ln \left( \frac{\dot{\epsilon}}{0.05/\text{min}} \right) \right] \exp[0.01581(T - 21.5^\circ\text{C})]$$

For 40 w% talc-filled polypropylene in the L direction:

$$m = 1.1898$$

$$\beta(1/\text{MPa}) = 0.07028 \left[ 1 - 0.004511 \ln \left( \frac{\dot{\epsilon}}{0.05/\text{min}} \right) \right] \exp[0.01179(T - 21.5^\circ\text{C})]$$

Table 2. Constitutive Parameters of 40 w% Talc-Filled Polypropylene.

Strain Rate (min <sup>-1</sup> )	Temp. (°C)	Parallel to the flow direction (L direction)				Normal to the flow direction (W direction)			
		<i>m</i> <sup>a</sup>	$\beta$ <sup>a</sup>	<i>m</i> <sup>b</sup>	$\beta$ <sup>b</sup>	<i>m</i> <sup>a</sup>	$\beta$ <sup>a</sup>	<i>m</i> <sup>b</sup>	$\beta$ <sup>b</sup>
0.05	21.5	1.1828	0.06167	1.1867	0.06294	1.3422	0.1539	1.1701	0.0765
0.5		1.2118	0.06559	1.2083	0.06498	1.1923	0.0748	1.1883	0.0752
5		1.1809	0.05752	1.1947	0.06070	1.2251	0.0813	1.1931	0.0506
0.05	50	1.1807	0.07962	1.1817	0.08289	1.1730	0.0854	1.1832	0.0923
0.5		1.1839	0.07663	1.1813	0.07717	1.2161	0.0963	1.1889	0.0866
5		1.1650	0.06822	1.1554	0.06514	1.1917	0.0860	1.2019	0.0871
0.05	75	1.1947	0.1075	1.2084	0.1442	1.2250	0.1060	1.2042	0.1879
0.5		1.2057	0.1092	1.2083	0.1323	1.2957	0.1114	1.2073	0.1688
5		1.2060	0.1009	1.2031	0.1010	1.3281	0.1144	1.2305	0.1661
0.05	100	1.3362	0.1390	1.2296	0.1691	1.2929	0.1384	1.2425	0.2294
0.5		1.2707	0.1076	1.2201	0.1493	1.2583	0.1218	1.2287	0.1997
5		1.2382	0.1071	1.2097	0.1289	1.2577	0.1142	1.2404	0.1788

<sup>a</sup>Based on Eqs 12 and 13. <sup>b</sup>Based on Eq 8.

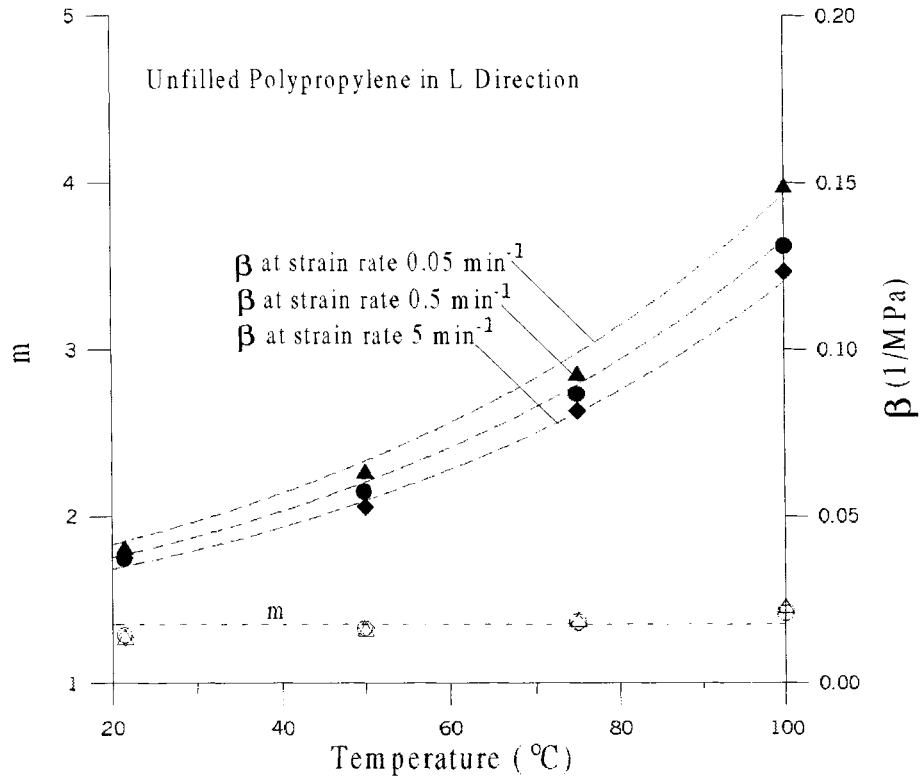


Fig. 6. Effect of temperature on compliance factor  $\beta$  and strain exponent  $m$  of unfilled polypropylene in the flow (L) direction.

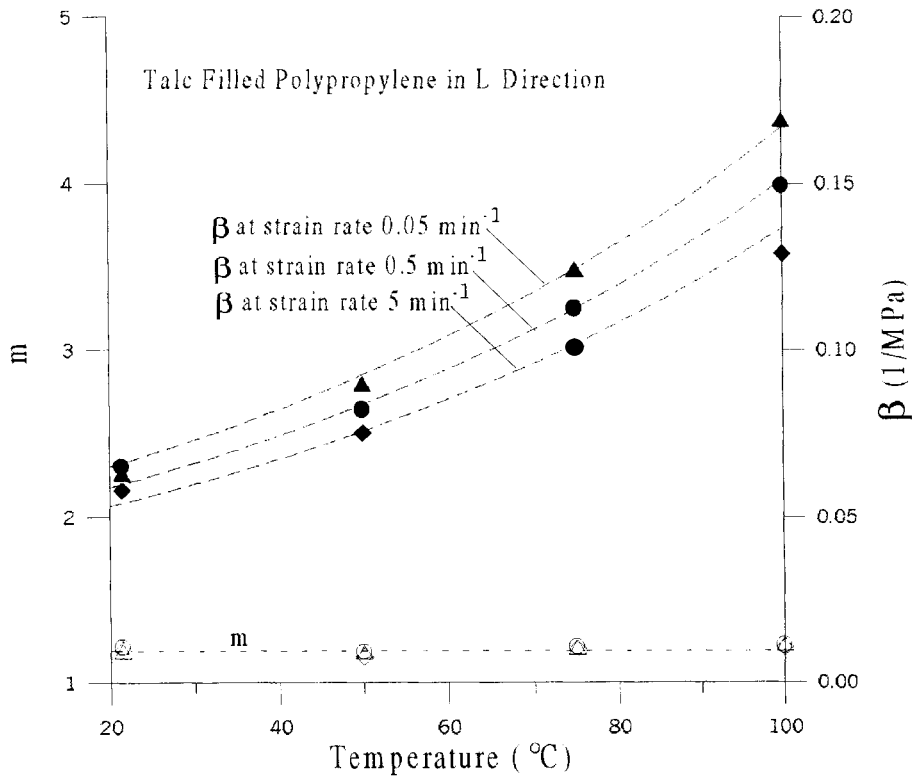


Fig. 7. Effect of temperature on compliance factor  $\beta$  and strain exponent  $m$  of 40 w% talc-filled polypropylene in the flow (L) direction.

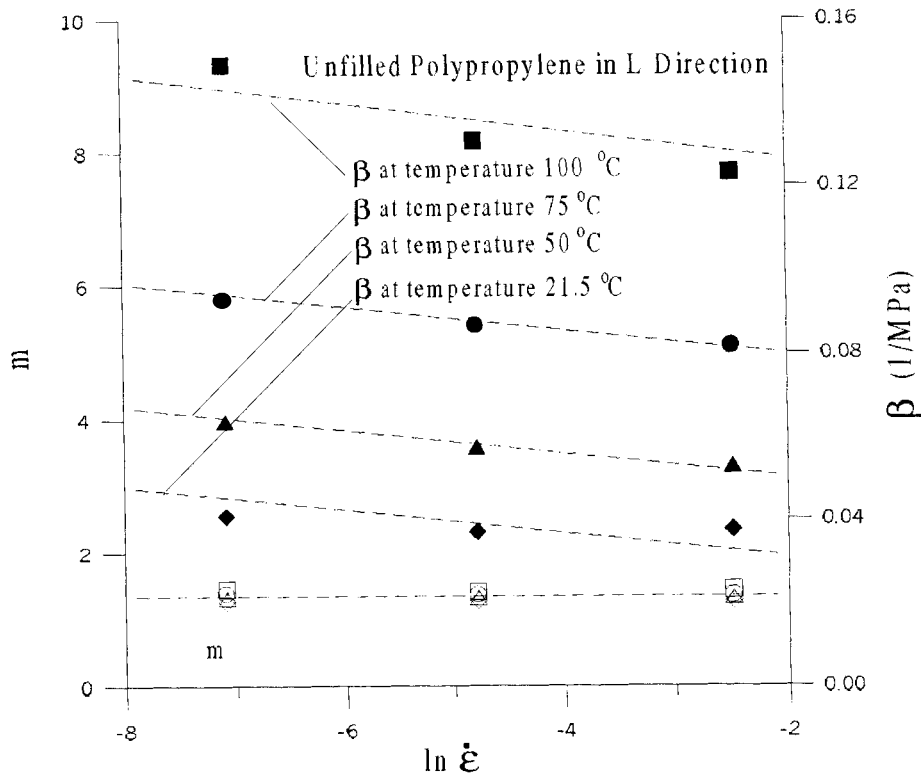


Fig. 8. Effect of strain rate on compliance factor  $\beta$  and strain exponent  $m$  of unfilled polypropylene in the flow (L) direction.

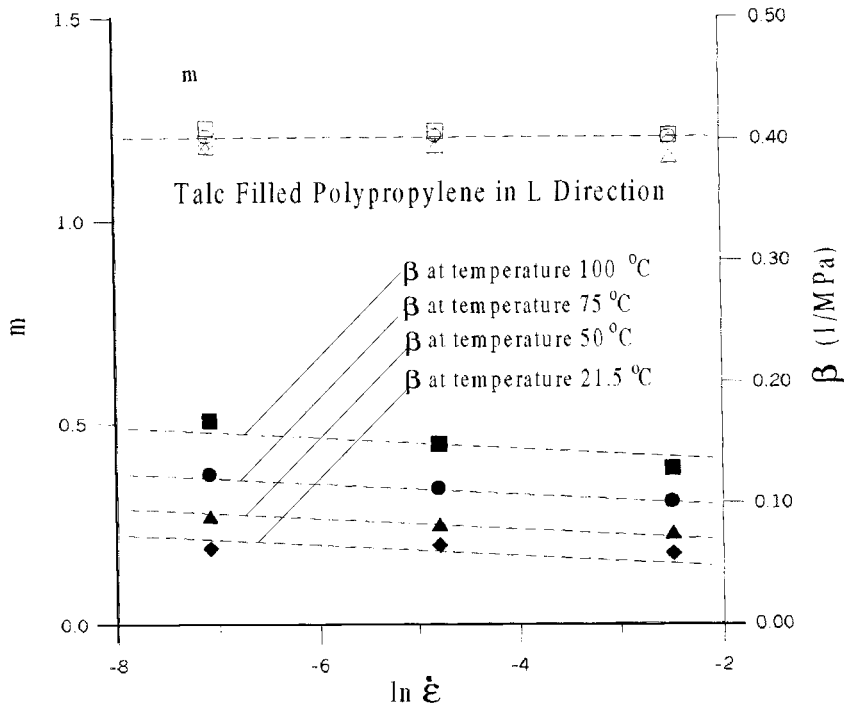


Fig. 9. Effect of strain rate on compliance factor  $\beta$  and strain exponent  $m$  of 40 wt% talc-filled polypropylene in the flow (L) direction.



For unfilled polypropylene in the W direction:

$$m = 1.3382$$

$$\beta(1/\text{MPa}) = 0.04700 \left[ 1 - 0.003463 \ln \left( \frac{\dot{\epsilon}}{0.05/\text{min}} \right) \right] \exp[0.01628(T - 21.5^\circ\text{C})]$$

For 40 w% talc-filled polypropylene in the W direction:

$$m = 1.2066$$

$$\beta(1/\text{MPa}) = 0.08226 \left[ 1 - 0.006808 \ln \left( \frac{\dot{\epsilon}}{0.05/\text{min}} \right) \right] \exp[0.01537(T - 21.5^\circ\text{C})]$$

In the above equations, reference strain rate and temperature are assumed to be  $0.05 \text{ min}^{-1}$  and  $21.5^\circ\text{C}$ , respectively. Substituting for elastic modulus  $E$ , compliance factor  $\beta$  and strain exponent  $m$  in Eq 4, the simulated stress-strain plots in the flow (L) direction are drawn as shown in Figs. 10 and 11, and they seem to fit the experimental data very well. The simulated stress-strain plots normal to the flow (W) direction (not included here) also show a very good agreement with the experimental data.

### 5. CONCLUSIONS

1. A three-parameter nonlinear constitutive model has been established to describe the strain rate and

temperature dependent behaviors of semi-crystalline polymers. The parameters in this model are the elastic modulus  $E$ , the strain exponent  $m$  and the compliance factor  $\beta$ . Effect of strain hardening (or strain softening) is controlled by strain component  $m$ . The flow stress level of the stress-strain curve is controlled by compliance parameter  $\beta$ .

2. The proposed constitutive equation fits the stress-strain diagrams of unfilled polypropylene and 40 w% talc-filled polypropylene, both of which exhibit strain softening characteristics after yielding. For these two materials,

- (a) The strain exponent  $m$ , is not only strain rate independent, but also temperature independent. The compliance parameter,  $\beta$ , on the other hand, decrease with strain rate and increase with temperature.
- (b) Talc filler decreases the strain exponent  $m$  and increases the compliance factor,  $\beta$ , which results in the flow stress level of 40 w% talc-filled polypropylene being lower than that of unfilled polypropylene.

### ACKNOWLEDGMENTS

The authors would like to acknowledge the financial support provided by the Ford Motor Company under its University Research Program to conduct this research.

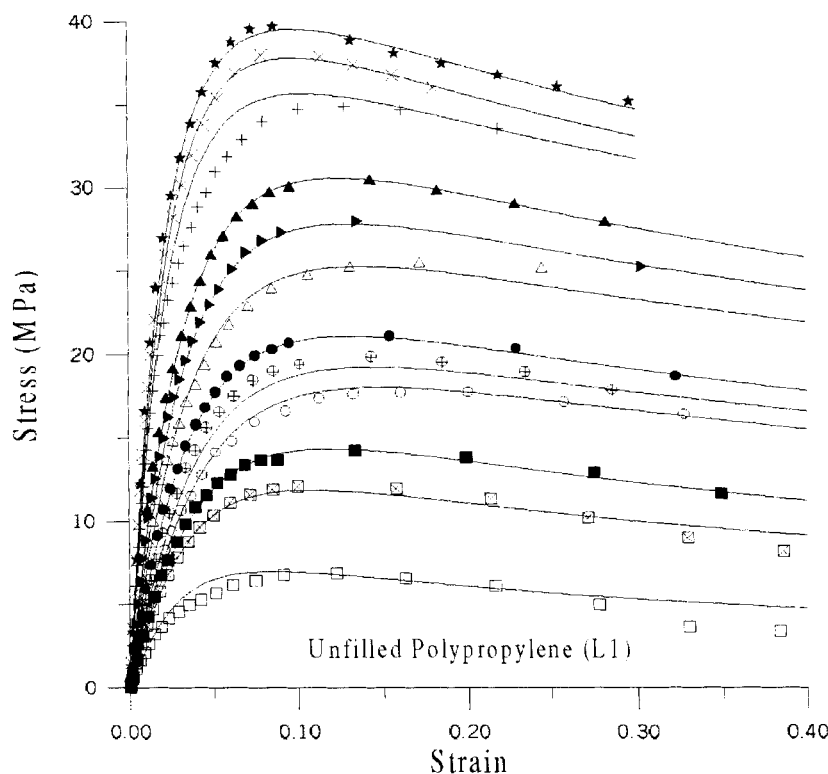


Fig. 10. Comparison of simulated stress-strain curves and experimental stress-strain curves of unfilled polypropylene in the flow (L) direction. +  $21.5^\circ\text{C}$ ,  $0.05 \text{ min}^{-1}$ ,  $\times$   $21.5^\circ\text{C}$ ,  $0.5 \text{ min}^{-1}$ ,  $\star$   $21.5^\circ\text{C}$ ,  $5 \text{ min}^{-1}$ ,  $\Delta$   $50^\circ\text{C}$ ,  $0.05 \text{ min}^{-1}$ ,  $\blacktriangleright$   $50^\circ\text{C}$ ,  $0.5 \text{ min}^{-1}$ ,  $\blacktriangle$   $50^\circ\text{C}$ ,  $5 \text{ min}^{-1}$ ,  $\circ$   $75^\circ\text{C}$ ,  $0.05 \text{ min}^{-1}$ ,  $\oplus$   $75^\circ\text{C}$ ,  $0.5 \text{ min}^{-1}$ ,  $\bullet$   $75^\circ\text{C}$ ,  $5 \text{ min}^{-1}$ ,  $\square$   $100^\circ\text{C}$ ,  $0.05 \text{ min}^{-1}$ ,  $\boxtimes$   $100^\circ\text{C}$ ,  $0.5 \text{ min}^{-1}$ ,  $\blacksquare$   $100^\circ\text{C}$ ,  $5 \text{ min}^{-1}$ .

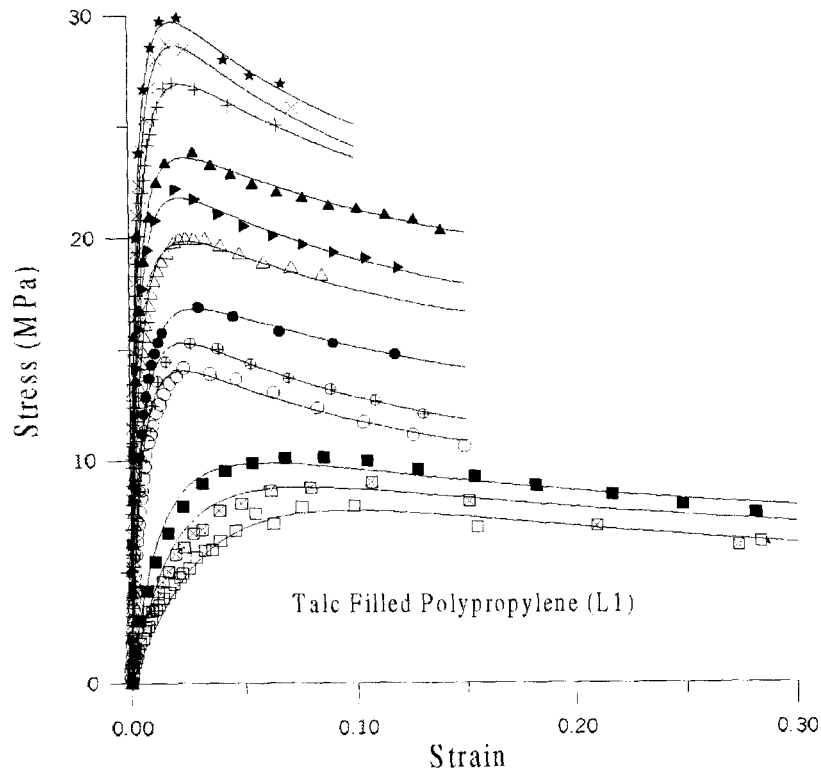


Fig. 11. Comparison of simulated stress-strain curves and experimental stress-strain curves of 40 w% talc-filled polypropylene in the flow (L) direction. The symbols are shown in Fig. 10.

The authors would also like to thank Dr. Y. Zhang, currently of Visteon, for sponsoring this research.

#### REFERENCES

1. B. Hartmann, G. F. Lee, and W. Wong, *Polym. Eng. Sci.*, **27**, 825 (1987).
2. E. M. Arruda, S. Ahzi, Y. Li, and A. Ganesan, *J. Eng. Matls. and Tech.*, **119**, 216 (1997).
3. P. Duffo, B. Monasse, J. M. Haudin, C. G'Sell, and A. Daghoun, *J. Matls. Sci.*, **30**, 701 (1995).
4. J. Amodeo and D. Lee, *Plastics and Plastic Composites: Material Properties, Part Performance and Process Simulation*, V. K. Stokes, ed., The American Society of Mechanical Engineers, New York (1991).
5. M. Kitagawa, T. Mori, and T. Matsutani, *J. Polym. Sci.: Part B: Polym. Phys.*, **27**, 85 (1989).
6. C. Zhang and I. D. Moore, *Polym. Eng. Sci.*, **37**, 414 (1997).
7. Y. Zhou and P. K. Mallick, *Polym. Eng. Sci.*, this issue.